 h the exception of pagination.

Battery-Based Energy Storage Transportation for Enhancing Power System Economics and Security

Yingyun Sun, *Member, IEEE*, Zuyi Li, *Senior Member, IEEE*, Mohammad Shahidehpour, *Fellow, IEEE*, and Bo Ai

***Abstract*—This paper evaluates the effect of integrating battery-based energy storage transportation (BEST) by railway transportation network on power grid operation and control. A time-space network model is adopted to represent transportation constraints. The proposed model integrates the hourly security-constrained unit commitment with vehicle routing problem. The BEST solution provides the locational and hourly charging/discharging schedule of the battery storage system. The mobility of BEST will be of particular interest for enhancing the power system resilience in disaster areas where the transmission grid is congested or on outrage. Two cases are used to simulate the BEST including a six-bus power system linking with a three-station railway system, as well as the IEEE 118-bus systems linking with an eight-station railway system. The results show that under certain conditions, the mobility of battery storage system can economically relieve the transmission congestion and lower the operation costs.**

***Index Terms*—Battery-based energy storage transportation (BEST), mixed-integer programming (MIP), security-constraint unit commitment (SCUC), time-space network (TSN).**

NOMENCLATURE

Indices and Sets

i, j	Index of buses.
ij	Index of arcs in time-space network (TSN) from station i to station j.
k	Index of battery-based energy storage transportation (BEST) trains.
l	Index of transmission lines.
s	Index of time spans.
t	Index of hours.
A	Set of arcs in a TSN at a single time span.
A_i^+	Set of arcs in a TSN which start from station i.
A_i^-	Set of arcs in a TSN which end at station i.
G	Set of generating units.
RS	Set of buses with railway stations.
T_s	Set of hours in time span s.

Constants

$C_{k,ij}$	Transportation cost of BEST k in arc ij.
DR_u	Ramp-down rate limit of unit u.
$E_{k,0}$	Initial energy stored in BEST k.
$E_{k,\mathrm{NS}}$	Terminal energy stored in BEST k.
$E_{\max,k}$	Maximum energy capacity of BEST k.
$E_{\min,k}$	Minimum energy capacity of BEST k.
$I_{k,i,0}$	Initial state of BEST k in station i.
$I_{k,i,\mathrm{NS}}$	Terminal state of BEST k in station i.
NS	Number of time spans.
NT	Number of hours.
$P_{D,t}$	Total system load at time t.
$P_{\max,k}$	Maximum power exchange rate of BEST k.
$P_{\max,l}$	Maximum capacity of line l.
$P_{\max,u}$	Maximum generation capacity of unit u.
$P_{\min,k}$	Minimum power exchange rate of BEST k.
$P_{\min,u}$	Minimum generation capacity of unit u.
SR_t	System spinning reserve requirement at time t.
$T_{\mathrm{OFF},u}$	Minimum OFF time requirement of unit u.
$T_{\mathrm{ON},u}$	Minimum ON time requirement of unit u.
UR_u	Ramp-up rate limit of unit u.

Variables

$F_{C,u}$	Fuel consumption function of unit u.
$I_{k,ij,s}$	Status of arc ij of BEST k at time span s.
$I_{u,t}$	Commitment status of unit u at time t.
$P_{k,i,t}$	Injected/absorbed power of BEST k at bus i and time t.
$P_{l,t}$	Real-power flow on line l at time t.
$P_{u,t}$	Generation of unit u at time t.
$\mathrm{SD}_{u,t}$	Shutdown cost of unit u at time t.
$\mathrm{SR}_{u,t}$	Spinning reserve of unit u at time t.
$\mathrm{SR}_{k,i,t}$	Spinning reserve of BEST k at bus i at time t.
$\mathrm{SU}_{u,t}$	Start-up cost of unit u at time t.
$X_{\mathrm{OFF},u,t}$	OFF time of unit u at time t.
$X_{\mathrm{ON},u,t}$	ON time of unit u at time t.
$y_{u,t}$	Startup indicator of unit u at time t.
$z_{u,t}$	Shutdown indicator of unit u at time t.

Manuscript received January 2, 2015; accepted January 2, 2015. This work was supported in part by the National Natural Science Foundation of China under Grant 50907034, and in part by the National Key Basic Research Program of China (973 Program) under Grant 2012CB215203. The work of Y. Sun was supported by the China Scholarship Council for a one-year sabbatical study in the Galvin Center at the Illinois Institute of Technology, Chicago, IL, USA. Paper no. TSG-00003-2015.

Y. Sun and B. Ai are with the State Key Laboratory of Alternate Electrical Power System with Renewable Energy Sources, North China Electric Power University, Beijing 102206, China (e-mail: sunyy@ncepu.edu.cn).

Z. Li is with the Robert W. Galvin Center for Electricity Innovation, Illinois Institute of Technology, Chicago, IL 60616 USA.

M. Shahidehpour is with the Robert W. Galvin Center for Electricity Innovation, Illinois Institute of Technology, Chicago, IL 60616 USA, and also with the Renewable Energy Research Group, King Abdulaziz University, Jeddah 22254, Saudi Arabia.

Digital Object Identifier 10.1109/TSG.2015.2390211

I. INTRODUCTION

THE POWER industry is experiencing unprecedented challenges as its primary source of energy is shifting from fossil fuel to renewable energy. To achieve this transformation,

 h the exception of pagination.

two major problems are: 1) how to transmit large sums of renewable energy from remote locations to load centers; and 2) how to accommodate the variability of renewable energy resources (RES) at load points.

The fast developing energy storage technology (EST) could offer a well-established approach for the two issues mentioned above [1]. ESTs are divided into four types for grid-scale applications, including mechanical, electrical, chemical, and thermal [2]. The mechanical storage, including pumped-hydro and compressed-air, accounts for 99% of the worldwide storage capacity, but strict locational requirements hinder their widespread developments for power system applications.

The battery-based energy storage (BES) technology represents an excellent, but rather expensive, EST for the integration of RES [3], [4]. BES offers a pollution-free operation with a long life cycle, low maintenance, high efficiency, and fast response time [5], [6]. In essence, BES has become one of the most promising technologies in grid-size storage applications, including load shifting [7], [8], managing RES variability [9], [10], enhancing the system stability [11], [12], and so on.

BES applications in electric vehicles (EVs) and the impact of its mobility on the electricity grid management were studied extensively [13]–[18]. In [13], the stochastic unit commitment model was adopted to study the impact of BES (aggregated EV fleets) and the renewable energy integration on the hourly thermal generation schedule. The mixed-integer programming (MIP)-based security-constrained unit commitment (SCUC) was used in [14] and [15] to study the impact of plug-in hybrid EV on the thermal generation reserve scheduling. The modular BES can also be installed in ships and trains where its mobility provides an alternative for transmitting electricity. The BES mobility in EVs was studied by applying SCUC in [16] and [17], in which the results show that the BES mobility can relieve transmission congestion and lower the hourly power production cost. However, additional research and implementation will be needed on this subject as frequent charging/discharging of BES in vehicle-to-grid (V2G) applications will lower the battery life significantly [18].

The BES mobility can support the major shift in the thermal power generation paradigm throughout the world. In the U.S. alone, large coal-fired power plants are subject to retirement. The coal usage for electric power generation is expected to fall to 14.7 quadrillion Btu in 2040 as compared with 18.7 quadrillion Btu in 2011 [19]. At the same time, there will be an additional capacity available on freight trains which were used for transporting coal to electric power plants. The lower usage of freight trains can provide the additional mobile capacity required for transporting the energy stored in modular BES along the train path from the rich wind energy zones to zones with the highest locational marginal prices in the country. Similar to V2G applications, the energy stored in modular BES installed on freight trains can be efficiently transported via rail to remote locations.

Such large utilizations of mobile BES would demonstrate five basic goals:

1) to optimize the power grid operation at the national level for delivering the surplus capacity to other locations where it is needed the most for local peak shaving;
2) to enhance the power system resilience by providing the rail-transport energy quickly to areas of the country which are inflicted by natural disaster;
3) to defer large investments on power transmission infrastructure by utilizing the BES mobility;
4) to capture the variable renewable energy and transmit it to regions where such energy has the highest potential for grid management;
5) to help individual states meet renewable portfolio standard compliance and greenhouse gas emission at regional levels;

This paper proposes an integrated model for the hourly SCUC which utilizes the BES transportation by railway (referred to as BEST) for V2G-type applications. The integrated SCUC solution will provide the locational and hourly charging/discharging schedule of BEST for minimizing the power system operation cost. The BEST application in SCUC will take into consideration thermal unit constraints, power transmission constraints, BEST charging/discharging constraints, and BEST transportation constraints.

The contributions of this paper include the following.

1) The TSN-based BEST model is integrated into the SCUC model, which combines transportation and electrical constraints for an optimal operation of electric power and transportation systems.
2) The proposed model is used to study the impact of BEST on the hourly generation schedule of thermal units in power systems.
3) The proposed model provides an analysis of the base station and transportation cost on the mobility of BEST.

The rest of this paper is organized as follows. Section II provides the mathematical model of BEST. The complete model of SCUC with BEST is given in Section III. Section IV presents two case studies with detailed discussion. The conclusion drawn from this paper is provided in Section V.

II. BEST Model

The railway system in many parts of the world is the most accessible, utilized, and complex means of transportation system. Every day, millions of passengers across the globe are transported via regional railway networks. To minimize the transportation cost, railway operators would schedule the trains using a classic optimization problem called vehicle routing problem (VRP) [20].

In this paper, the BEST locational and hourly charging/discharging schedule is embedded into the SCUC solution, which is a nondeterministic polynomial-time hard (NP-hard) optimization problem. The hourly SCUC solution will also provide the best solution to the VRP with time windows (VRPTW) [21], [22]. A TSN is used to model the railway transportation system. TSN has been used in VRPTW for airline scheduling [23]. It has also been extended to multidepot bus scheduling and vehicle and crew scheduling [24], [25].

 h the exception of pagination.

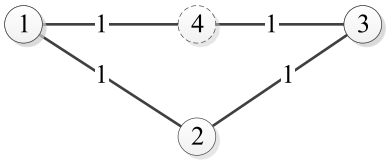

Fig. 1. Illustration of a railway network with travel times.

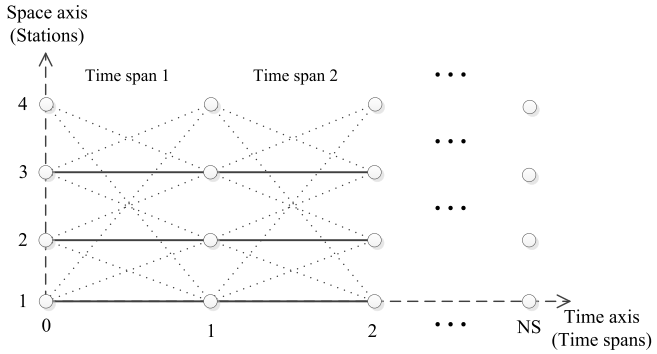

Fig. 2. Illustration of TSN.

A. TSN-Based BEST Model

A TSN along the time horizon is established in our model by representing railway stations equipped with charging/discharging devices. In this section, we use a small example to illustrate how a TSN is modeled for a physical railway network.

Consider a small railway network in Fig. 1 with three stations {1, 2, 3}, in which the number on each line that connects two stations represents the travel time, stated in time spans, between the two stations. One time span can be any number of hours stated as input to TSN. In Fig. 1, the travel time between stations 1 and 3 is two time spans and twice that between the other stations. To simplify the problem, a virtual station 4 is added between stations 1 and 3 so that the travel times between any two stations would be equal to one time span. The designated travel time between any two stations in Fig. 1 is an important parameter in TSN. A small time span will increase the complexity of the TSN model with the introduction of multiple virtual stations, while a large time span will reduce the accuracy of the TSN model. A practical TSN would represent a compromise between accuracy and problem size.

The TSN shown in Fig. 2 depicts the possible hourly connections in the augmented railway network with four stations shown in Fig. 1. The vertical axis in Fig. 2 represents railway stations and the horizontal axis represents the hourly scheduling horizon. In Fig. 2, nodes and arcs represent the two major components in TSN. Each node represents a railway station (real or virtual) in the scheduling horizon, and an arc represents a possible link between any two stations in the given time horizon.

In this paper, there are two types of arcs in TSN. The first type, horizontal solid arcs in Fig. 2, represents the BEST stop for exchanging power at any station that is connected to the power grid. An arc of this type is referred to as the grid-connecting arc. The second type, sloped dotted arcs in Fig. 2, represents the BEST transportation between stations in any given period of time. An arc of this type is referred to as the transporting arc. It is noteworthy that physical stations can be connected to both types of arcs, while virtual stations can only be connected to transporting arcs. Furthermore, the railway stations without charging/discharging devices are treated as virtual stations, because BEST cannot be connected to the power grid in such stations.

In the TSN model, the BEST state representation in a time span, which is the most difficult part for setting up the connection-based model in VRPTW, is configured as arcs [20].

B. Mathematical Formulation of TSN-Based BEST Model

In TSN, BEST can be modeled as follows:

$$\sum_{ij\in A} I_{k,ij,s} = 1, \quad \forall s, \forall k \tag{1}$$

$$\sum_{ij\in A_i^+} I_{k,ij,s+1} = \sum_{ij\in A_i^-} I_{k,ij,s}, \forall s = 1, \cdots \mathrm{NS}-1, \quad \forall i, \forall k \tag{2a}$$

$$\sum_{ij\in A_i^+} I_{k,ij,1} = I_{k,i,0}, \quad \forall i, \forall k \tag{2b}$$

$$\sum_{ij\in A_i^-} I_{k,ij,\mathrm{NS}} = I_{k,i,\mathrm{NS}}, \quad \forall i, \forall k. \tag{2c}$$

Equation (1) represents BEST state constraints. Each BEST k can only be on one arc in time span s. Equation (2) represents BEST connection constraints. In (2a), each BEST k in station i at the end of time span s is in node (i, s) in the TSN, which means that, in the next time span $s+1$, BEST k must be in one of the arcs which start from node (i, s). If we treat the arcs connecting the nodes as flows, this means the in and out flows of each node in the TSN must be equal. In particular, in (2b) for time span 1, the outflow at each station must be equal to the initial state of BEST k, and in (2c) for the last time span NS, the inflow of each station must be equal to the terminal state of BEST k.

Other BEST constraints include

$$I_{k,ii,s}P_{\min,k} \le P_{k,i,t} \le I_{k,ii,s}P_{\max,k}, \forall t \in T_s, \forall s, \forall k, \forall i \tag{3}$$

$$E_{\min,k} \le E_{k,t} \le E_{\max,k}, \forall t, \forall k \tag{4}$$

$$E_{k,t} = E_{k,t-1} + \sum_i P_{k,i,t}, \forall t, \forall k \tag{5}$$

$$E_{k,t} = E_{k,\mathrm{NS}} \quad t = \mathrm{NS}, \forall k. \tag{6}$$

The BEST charging/discharging power constraints are given in (3). BEST k charges from the grid when $P_{k,i,t} > 0$ and discharges to the grid when $P_{k,i,t} < 0$. Note that, $P_{\min,k}$ is negative. As mentioned before, a BEST state can only exchange power with the grid when it is in horizontal TSN arcs, which means that the BEST stops at a certain station when it is connected to the grid at that station. The BEST energy capacity constraints are given in (4). The BEST energy balance constraints are given in (5). The BEST terminal energy capacity constraints are given in (6).

III. SCUC Formulation With BEST

The SCUC model with BEST is described as follows.

 h the exception of pagination.

A. Objective Function of SCUC

The objective function (7), which is the overall cost, is composed of two parts. The first part is the total power production cost which includes fuel costs for producing electric power and startup and shutdown costs of individual units over the scheduling horizon. The second part is the total BEST transportation cost

$$\min \sum_{t} \sum_{u \in G} \left[F_{C,u}\left(P_{u,t}\right) + \mathrm{SU}_{u,t} + \mathrm{SD}_{u,t} \right] + \sum_{k} \sum_{s} C_{k,ij} I_{k,ij,s}. \tag{7}$$

B. Power Grid System Constraints

Equation (8) is the system power balance constraint and (9) is the system spinning reserve constraint. BEST k can only be connected to the grid when it is on a grid-connecting arc, that is $I_{k,ii,s} = 1$

$$\sum_{u \in G} P_{u,t} - \sum_{k} \sum_{i \in \mathrm{RS}} P_{k,i,t} = P_{D,t} \quad \forall t \tag{8}$$

$$\sum_{u \in G} \mathrm{SR}_{u,t} + \sum_{k} \sum_{i \in \mathrm{RS}} \mathrm{SR}_{k,i,t} \geq \mathrm{SR}_{t}, \quad \forall t \tag{9}$$

where

$$\mathrm{SR}_{u,t} = \begin{cases} P_{\max,u} - P_{u,t}, & \text{if unit } u \text{ is ON at hour } t \\ 0, & \text{if unit } u \text{ is OFF at hour } t \end{cases}$$

$$\mathrm{SR}_{k,i,t} = \begin{cases} P_{\max,k} - P_{k,i,t}, & \text{if } I_{k,ii,s} = 1 \\ 0, & \text{if } I_{k,ii,s} = 0 \end{cases} \quad \forall t \in T_s.$$

C. Thermal Unit Constraints

The thermal unit constraints include capacity limits of generating units (10), ramping up limits (11), ramping down limits (12), minimum ON time limits (13), and minimum OFF time limits (14), etc. The detailed modeling of individual generating unit constraints is given in [26]

$$P_{\min,u} I_{u,t} \leq P_{u,t} \leq P_{\max,u} I_{u,t} \quad \forall u, \forall t \tag{10}$$

$$P_{u,t} - P_{u,t-1} \leq \mathrm{UR}_{u}(1 - y_{u,t}) + P_{\min,u} y_{u,t} \quad \forall u, \forall t \tag{11}$$

$$P_{u,t-1} - P_{u,t} \leq \mathrm{DR}_{u}(1 - z_{u,t}) + P_{\min,u} z_{u,t} \quad \forall u, \forall t \tag{12}$$

$$\sum_{t=1}^{\mathrm{UT}_u} \left(1 - I_{u,t}\right) = 0 \quad \forall u, \forall t \tag{13a}$$

$$\sum_{\tau=t}^{t+T_{\mathrm{ON},u}-1} I_{u,\tau} \geq T_{\mathrm{ON},u} y_{u,t} \quad \forall t = \mathrm{UT}_u + 1, \ldots, \mathrm{NT} - T_{\mathrm{ON},u} + 1 \tag{13b}$$

$$\sum_{\tau=t}^{\mathrm{NT}} \left(I_{u,\tau} - y_{u,t}\right) \geq 0 \quad \forall t = \mathrm{NT} - T_{\mathrm{ON},u} + 2, \ldots, \mathrm{NT} \tag{13c}$$

$$\sum_{t=1}^{\mathrm{DT}_u} I_{u,t} = 0 \quad \forall u, \forall t \tag{14a}$$

$$\sum_{\tau=t}^{t+T_{\mathrm{OFF},u}-1} \left(1 - I_{u,\tau}\right) \geq T_{\mathrm{OFF},u} y_{u,t} \quad \forall t = \mathrm{DT}_u + 1, \ldots, \mathrm{NT} - T_{\mathrm{OFF},u} + 1 \tag{14b}$$

$$\sum_{\tau=t}^{\mathrm{NT}} \left(1 - I_{u,\tau} - z_{u,t}\right) \geq 0 \quad \forall t = \mathrm{NT} - T_{\mathrm{OFF},u} + 2, \ldots, \mathrm{NT} \tag{14c}$$

$$y_{u,t} - z_{u,t} = I_{ut} - I_{u(t-1)} \tag{15}$$

$$y_{ut} + z_{ut} \leq 1 \tag{16}$$

where

$$\mathrm{UT}_u = \max\left\{0, \min\left[\mathrm{NT}, \left(T_{\mathrm{ON},u} - X_{\mathrm{ON},u,0}\right) I_{u,0}\right]\right\}$$

$$\mathrm{DT}_u = \max\left\{0, \min\left[\mathrm{NT}, \left(T_{\mathrm{OFF},u} - X_{\mathrm{OFF},u,0}\right)\left(1 - I_{u,0}\right)\right]\right\}.$$

D. Power Grid Line Flow Constraints

The shift factor method [27] is adopted for representing power grid transmission line flow constraints in (17)

$$-P_{\max,l} \leq P_{l,t} \leq P_{\max,l}, \quad \forall t, \forall l. \tag{17}$$

E. BEST Constraints

Equations (1)–(6) are used for representing the BEST constraints.

IV. Case Studies

In this section, a six-bus power system and the IEEE 118-bus power system are used to demonstrate the impact of BEST on power system operation. All cases are solved by Gurobi [28] in a Windows 2003 Server R2 (CPU: 8 Core Xeon 2.4 G Hz, RAM: 64 G).

A. BEST Data

In this paper, the sodium-sulphur (NaS) battery technology is adopted for BEST. NaS is a new promising high temperature battery technology, which is highly energy efficient (89% or more) and is made from inexpensive and nontoxic materials [3], [29]. We could equally apply any other type of batteries for the BEST application including sodium-nickel-chloride, Vanadium Redox, lead-acid, and so on [29].

In this paper, we assume that NaS batteries offer energy and power densities at 200 W/kg and 100 W/Kg, respectively. We also assume that a 50-feet standard railway car can load 100 tons of cargo; so each car carrying NaS batteries would carry $100 \times 10^3 \times 200 \times 10^{-6} = 20$ MWh with specific power of $100 \times 10^3 \times 100 \times 10^{-6} = 10$ MW.

B. Six-Bus Power System Case Study

A six-bus power system and the corresponding railway network are shown in Fig. 3. The characteristics of generating units, buses, transmission lines, and hourly loads over the 24 h horizon are given in Tables V–IX in the Appendix. We assume that there are three railway stations (1, 4, 5) with integrated BEST devices. The trip between any two stations will take 2 h; so a 2 h time span is adopted here. In this case study, BEST includes one locomotive and six railway cars. So the BEST energy and power in this case are 120 MWh and 60 MW, respectively.

 h the exception of pagination.

TABLE I
BEST ROUTE IN CASE 1

	Overall cost: $82,526.23											
Time span (0-24)	0-2	2-4	4-6	6-8	8-10	10-12	12-14	14-16	16-18	18-20	20-22	22-24
Position of BEST	1-1	1-1	1-1	1-1	1-4	4-4	4-4	4-4	4-4	4-4	4-4	4-1
Status of BEST	Charging				Transporting			Discharging				Transporting

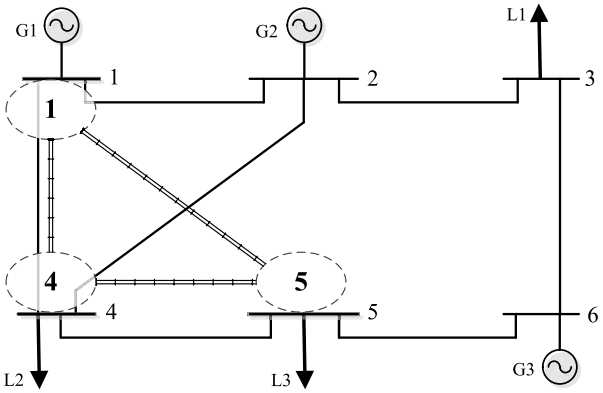

Fig. 3. Railway network of the six-bus three-station system.

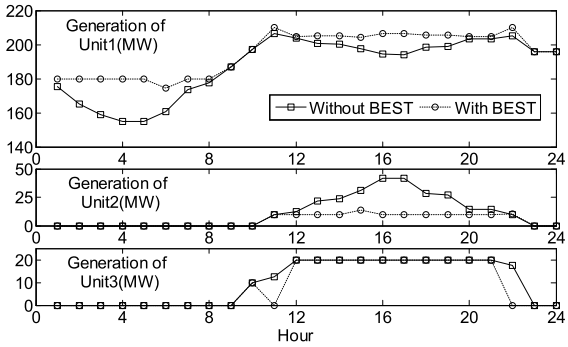

Fig. 4. Hourly dispatch of units 1–3 with/without BEST.

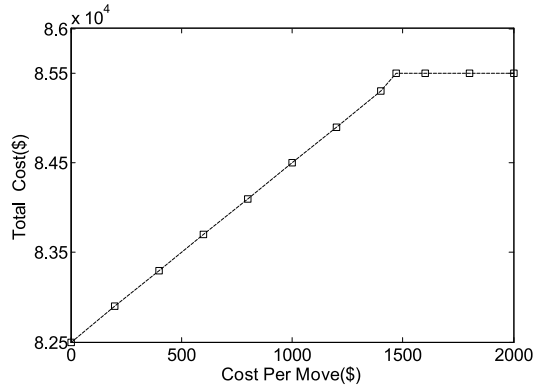

Fig. 5. Impact of transportation cost on the overall cost.

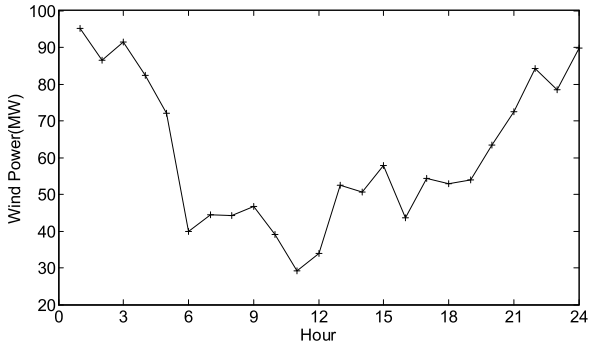

Fig. 6. Twenty-four hourly wind farm active power.

1) Case 1: Impact of BEST on the Hourly SCUC: In this case, the BEST base station is at bus 1 and the transportation cost at each trip between two stations is initially assumed to be 0. Accordingly, the daily operating cost of power system with BEST is $82 526.23, which is $2968.00 less than that without BEST. Fig. 4 shows the hourly dispatch of units 1–3 in which BEST would reshape the power system load profile. Unit 3 in Fig. 4 is shut down at hours 11 and 22 to minimize the total operating cost. The overall cost is reduced because the cheapest unit 1 is dispatched more in two periods of hours 1–7 and hours 11–20 for lowering the dispatch of the two expensive units 2 and 3.

Table I shows the BEST route. The BEST starts charging at bus 1 in the first four time spans (0:00–8:00) and travels via rail from bus 1 to bus 4 in time span 5 (8:00–10:00). The BEST starts discharging at bus 4 in the next six time spans (10:00–22:00), and returns to its base station via the railway 4–1 at the last time span of the day (22:00–24:00).

Fig. 5 shows the relationship between the overall cost given in (7) and the transportation cost per trip between two BEST stations. Here, the overall cost will remain unchanged once the trip cost hits $1471.21, which means that BEST will stay at its base station (bus 1) and act as a stationary energy storage if the transportation cost is high.

2) Case 2: Renewable Energy Integration: In this case, a 100 MW wind farm is connected to the power grid at bus 1 with a 24 h wind power profile shown in Fig. 6. The transportation cost for each trip between two stations is $200. Three scenarios are tested in this case.

1) *Scenario 1:* BEST base station at bus 1.
2) *Scenario 2:* BEST base station at bus 4.
3) *Scenario 3:* Fixed BES at bus 4.

Table II gives the BEST route and the overall cost in each scenario. The lowest cost is that of scenario 2 in which the BEST first travels to bus 1, where the wind farm is located, and once totally charged, it travels back to bus 4 for discharging. In this case, the fixed BES at bus 4 dose not perform well due to the congestion on the line between buses 1 and 4, which would limit the full utilization of the wind energy.

C. 118-Bus Power System

A modified IEEE 118-bus system, which includes 54 units, 186 branches, and 91 loads, is used in this case study. The peak load of the system is 3307.1 MW and the test data are provided at motor.ece.iit.edu/data/SCUC_118test.xls. Fig. 7 shows the

 h the exception of pagination.

TABLE II
BEST ROUTE IN CASE 2

Scenario	Time Span (0-24)												Overall cost ($)
	0-2	2-4	4-6	6-8	8-10	10-12	12-14	14-16	16-18	18-20	20-22	22-24	
1	1-1	1-1	1-4	4-4	4-4	4-4	4-4	4-4	4-4	4-1	1-1	1-1	76,848.79
2	4-1	1-1	1-4	4-4	4-4	4-4	4-4	4-4	4-4	4-4	4-4	4-4	76,512.56
3	4-4	4-4	4-4	4-4	4-4	4-4	4-4	4-4	4-4	4-4	4-4	4-4	76,955.19

TABLE III
BEST ROUTE IN CASE 3

	Overall cost: $813,533.10							
Time span (0-24)	0-3	3-6	6-9	9-12	12-15	15-18	18-21	21-24
Position of BEST	117-25	25-83	83-83	83-83	83-77	77-77	77-38	38-117
Status of BEST	T	T	C	C	T	D	T	T

TABLE IV
BEST ROUTE IN CASE 4

	Overall cost: $813,145.50							
Time span (0-24)	0-3	3-6	6-9	9-12	12-15	15-18	18-21	21-24
Position of BEST 1	117-25	25-83	83-83	83-83	83-77	77-77	77-38	38-117
Status of BEST 1	T	T	C	C	T	D	T	T
Position of BEST 2	69-77	77-77	77-77	77-83	83-83	83-77	77-77	77-69
Status of BEST 2	T	T	C	D	C	T	D	T

T: Transporting; C: Charging; D: Discharging;

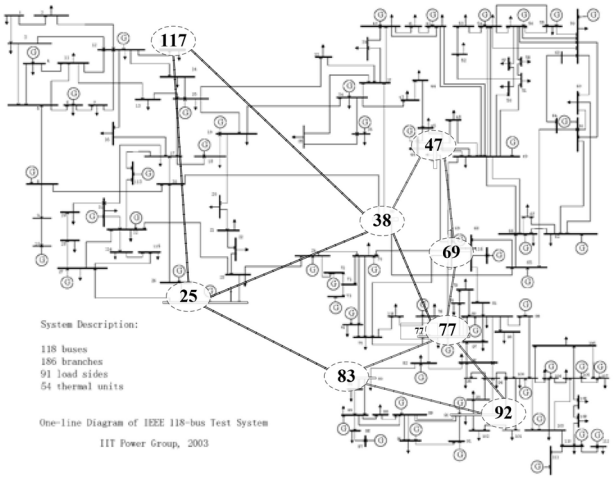

Fig. 7. Railway network in the modified IEEE 118-bus system.

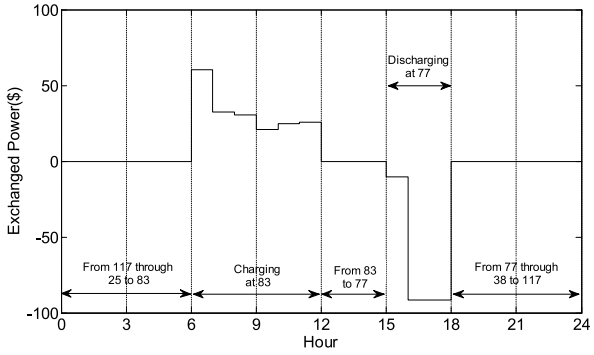

Fig. 8. Charging/discharging curve of BEST in case 3.

eight railway stations (at buses 25, 38, 47, 69, 77, 83, 92, 117) and the corresponding railway network. We assume the train travel time between any two stations that are connected directly by the railway is 3 h, so the time span is set as 3 h. The transportation cost is initially assumed to be zero. In this example, BEST includes one locomotive and ten cars with a total energy and power of 200 MWh and 100 MW, respectively.

1) Case 3: One BEST System With the Base Station at Bus 117: The overall cost of Case 3 with BEST is $813 533.10, which is $598.90 less than the cost without BEST. Fig. 8 gives the BEST charging/discharging profile, and Table III shows the BEST transportation route. In the first two time spans (0:00–6:00), the BEST travels from station 117 through station 25 to station 83. It is charged at the following two time spans (6:00–12:00) before traveling to station 77 at time span 5 (12:00–15:00). After discharging in time span 6 (15:00–18:00), BEST returns to its base station in the last two time spans (18:00–24:00). The BEST chooses a different path when traveling back to its base station (77-38-117), which is shorter than its outbound path to station 77 (117-25-83-77).

2) Case 4: Two BEST Systems With Base Stations at Buses 117 and 69: In this case, two BEST systems are considered in the railway network: BEST 1 and BEST 2. The base stations for BEST 1 and BEST 2 are at buses 117 and 69, respectively. The overall cost with BESTs in case 4 is $813 145.50, which is $986.50 less than that without BEST and $387.60 less than that in case 3. Figs. 9 and 10 show the charging/discharging profile of the two BEST systems, respectively. Table IV shows the BEST status and the optimal transportation route.

The route of BEST 1 is exactly the same as that in case 3, but the exchanged power is slightly different. BEST 2 first travels to station 83 through station 77 in the first two time spans (0:00–6:00), and exchanges power with the grid in the following three time spans: 1) charging first (6:00–9:00); 2) then discharging (9:00–12:00); and 3) charging again (12:00–15:00). This is because of the load profile in this period. BEST 2 continues its travel to station 77 where it

 h the exception of pagination.

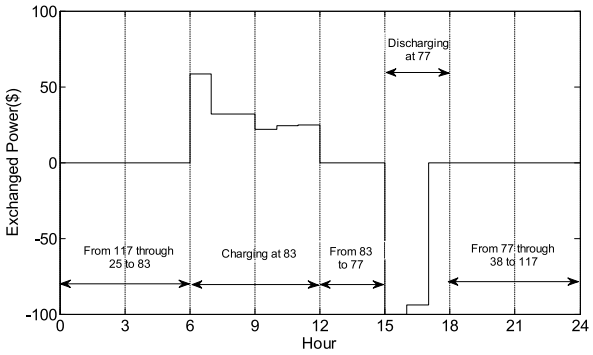

Fig. 9. Charging/discharging curve of BEST 1 in case 4.

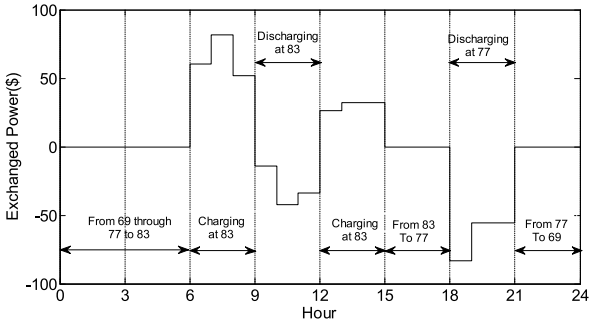

Fig. 10. Charging/discharging curve of BEST 2 in case 4.

is discharged at 18:00–21:00, and finally returns to its base station at the last time span (21:00–24:00).

V. Conclusion

In this paper, the impact of mobile BES on power grid operations is evaluated. The proposed model integrates TSN and SCUC models to prescribe the optimal scheduling of generating units and the locational and hourly charging/discharging schedule of the BEST. The proposed BEST solution provides the optimal train travel route as well. The numerical tests on the six-bus power system linked with the three-station railway system and the IEEE 118-bus systems linked with the eight-station railway system demonstrate the effectiveness of the proposed model.

The simulation results show that BEST can reduce the grid operation cost and the congestion in the power grid by two ways: 1) by peak load shaving; and 2) grid congestion relief by railway transportation. Furthermore, in the case of large sums of renewable energy connected to a relatively weak grid, BEST can effectively transfer the renewable energy and relieve congestion simultaneously. The optimal BEST solution is available only when the transportation cost is less than the congestion cost, which is reduced by the BEST transportation.

We will continue the proposed work in our future studies in which the efficiency of battery charging/discharging in the renewable energy integration will be fully considered. Furthermore, when the proposed model is applied to larger scale electricity and transportation systems for analysis, the model could be too complex to be solved as a single MIP problem. The proposed work considering the application of decomposition technologies such as Benders decomposition and Lagrangian relaxation is currently under study.

Appendix

TABLE V
Parameters of Generators

Unit	Bus No.	Pmax (MW)	Pmin (MW)	Ini. State (h)	Min Off (h)	Min On (h)
G1	1	220	100	4	4	4
G2	2	100	10	2	3	2
G3	6	20	10	-1	1	1

TABLE VI
Parameters of Generators

Unit	Quadratic Unit Cost Coefficients			Startup Cost ($)	Shutdown Cost ($)
	a ($/MW^{2}h)	b ($/MWh)	c ($/h)		
G1	0.004	13.5	179.6	180	50
G2	0.001	32.6	129.9	360	40
G3	0.005	17.6	137.4	60	0

TABLE VII
Transmission Line Data

Line	From Bus	To Bus	X (p.u.)	Flow Limit (MW)
1	1	2	0.17	200
2	1	4	0.258	100
3	2	4	0.197	100
4	5	6	0.14	100
5	3	6	0.018	100
6	2	3	0.037	200
7	4	5	0.037	200

TABLE VIII
Hourly Load and Spinning Reserve

Hour	Load(MW)	Reserve(MW)	Hour	Load(MW)	Reserve(MW)
1	175.19	12.26	13	242.18	16.95
2	165.15	11.56	14	243.60	17.05
3	158.67	11.10	15	248.86	17.42
4	154.73	10.83	16	255.79	17.91
5	155.06	10.85	17	256.00	17.92
6	160.48	11.23	18	246.74	17.27
7	173.39	12.14	19	245.97	17.22
8	177.60	13.33	20	237.35	16.62
9	186.81	14.39	21	237.31	16.62
10	206.96	15.20	22	232.67	15.90
11	228.61	16.00	23	195.93	14.07
12	236.10	16.52	24	195.60	13.78

TABLE IX
Bus Load

Name	Bus No.	Load Percentage (%)
L1	3	20
L2	4	40
L3	5	40

References

[1] J. P. Barton and D. G. Infield, "Energy storage and its use with intermittent renewable energy," *IEEE Trans. Energy Convers.*, vol. 19, no. 2, pp. 441–448, Jun. 2004.

[2] H. Chen *et al.*, "Progress in electrical energy storage system: A critical review," *Prog. Nat. Sci.*, vol. 19, no. 3, pp. 291–312, Mar. 2009.

 h the exception of pagination.

[3] S. Koohi-Kamali, V. V. Tyagi, N. A. Rahim, N. L. Panwar, and H. Mokhlis, "Emergence of energy storage technologies as the solution for reliable operation of smart power systems: A review," *Renew. Sustain. Energy Rev.*, vol. 25, pp. 135–165, Sep. 2013.
[4] K. C. Divya and J. Østergaard, "Battery energy storage technology for power systems—An overview," *Elect. Power Syst. Res.*, vol. 79, no. 4, pp. 511–520, Apr. 2009.
[5] A. A. Akhil *et al.*, DOE/*EPRI 2013 Electricity Storage Handbook*, Sandia Nat. Lab., Albuquerque, NM, USA.
[6] B. Dunn, H. Kamath, and J. M. Tarascon, "Electrical energy storage for the grid: A battery of choices," *Science*, vol. 334, no. 6058, pp. 928–935, 2011.
[7] M. Khodayar and M. Shahidehpour, "Cutting campus energy costs with hierarchical control: The economical and reliable operation of a microgrid," *IEEE Elect. Mag.*, vol. 1, no. 1, pp. 40–56, Sep. 2013.
[8] M. Parvania, M. Fotuhi-Firuzabad, and M. Shahidehpour, "Comparative hourly scheduling of centralized and distributed storage in day-ahead markets," *IEEE Trans. Sustain. Energy*, vol. 5, no. 3, pp. 729–737, Jul. 2014.
[9] S. M. Borba, A. Szklo, and R. Schaeffer, "Plug-in hybrid electric vehicles as a way to maximize the integration of variable renewable energy in power systems: The case of wind generation in northeastern Brazil," *Energy*, vol. 37, no. 1, pp. 469–481, 2012.
[10] M. Khodayar and M. Shahidehpour, "Stochastic price-based coordination of intra-hour wind energy and storage in a generation company," *IEEE Trans. Sustain. Energy*, vol. 4, no. 3, pp. 554–562, Jul. 2013.
[11] H. Yang, C. Y. Chung, and J. Zhao, "Application of plug-in electric vehicles to frequency regulation based on distributed signal acquisition via limited communication," *IEEE Trans. Power Syst.*, vol. 28, no. 2, pp. 1017–1026, May 2013.
[12] S. Han, S. Han, and K. Sezaki, "Development of an optimal vehicle-to-grid aggregator for frequency regulation," *IEEE Trans. Smart Grid*, vol. 1, no. 1, pp. 65–72, Jun. 2010.
[13] C. Liu, J. Wang, A. Botterud, Y. Zhou, and A. Vyas, "Assessment of impacts of PHEV charging patterns on wind-thermal scheduling by stochastic unit commitment," *IEEE Trans. Smart Grid*, vol. 3, no. 2, pp. 675–683, Jun. 2012.
[14] I. Krad and D. W. Gao, "Impact of PHEV on reserve scheduling: A MILP-SCUC method," in *Proc. North Amer. Power Symp. (NAPS)*, Manhattan, KS, USA, Sep. 2013, pp. 1–6.
[15] Z. Hu, S. Zhang, F. Zhang, and H. Lu, "SCUC with battery energy storage system for peak-load shaving and reserve support," in *Proc. IEEE Power Energy Soc. Gen. Meeting (PES)*, Vancouver, BC, Canada, Jul. 2013, pp. 1–5.
[16] M. E. Khodayar, L. Wu, and M. Shahidehpour, "Hourly coordination of electric vehicle operation and volatile wind power generation in SCUC," *IEEE Trans. Smart Grid*, vol. 3, no. 3, pp. 1271–1279, Sep. 2012.
[17] M. E. Khodayar, L. Wu, and Z. Li, "Electric vehicle mobility in transmission-constrained hourly power generation scheduling," *IEEE Trans. Smart Grid*, vol. 4, no. 2, pp. 779–788, Jun. 2013.
[18] C. Zhou, K. Qian, M. Allan, and W. Zhou, "Modeling of the cost of EV battery wear due to V2G application in power systems," *IEEE Trans. Energy Convers.*, vol. 26, no. 4, pp. 1041–1050, Dec. 2011.
[19] (Apr. 2013). *Energy Information Administration, Annual Energy Outlook*. [Online]. Available: http://www.eia.gov/forecasts/aeo/index.cfm
[20] S. Bunte and N. Kliewer, "An overview on vehicle scheduling models," *Public Transp.*, vol. 1, no. 4, pp. 299–317, 2009.
[21] M. R. Garey and D. S. Johnson, *Computers and Intractability: A Guide to the Theory of NP-Completeness*. San Francisco, CA, USA: W. H. Freeman, 1979.
[22] M. W. Savelsbergh, "Local search in routing problems with time windows," *Ann. Oper. Res.*, vol. 4, no. 1, pp. 285–305, 1985.
[23] C. A. Hane *et al.*, "The fleet assignment problem: Solving a large-scale integer program," *Math. Program.*, vol. 70, nos. 1–3, pp. 211–232, 1995.
[24] N. Kliewer, T. Mellouli, and L. Suhl, "A time-space network based exact optimization model for multi-depot bus scheduling," *Eur. J. Oper. Res.*, vol. 175, no. 3, pp. 1616–1627, 2006.
[25] N. Kliewer, B. Amberg, and B. Amberg, "Multiple depot vehicle and crew scheduling with time windows for scheduled trips," *Public Transp.*, vol. 3, no. 3, pp. 213–244, 2012.
[26] Y. Fu, M. Shahidehpour, and Z. Li, "Security-constrained unit commitment with AC constraints," *IEEE Trans. Power Syst.*, vol. 20, no. 2, pp. 1001–1013, Aug. 2005.
[27] M. Shahidehpour, H. Yamin, and Z. Li, *Market Operations in Electric Power Systems*. Hoboken, NJ, USA: Wiley, 2002.
[28] *Gurobi Optimizer Reference Manual,* Gurobi Optimization, Inc., Houston, TX, USA, 2014. [Online]. Available: http://www.gurobi.com
[29] R. Carnegie, D. Gotham, D. Nderitu, and P. V. Preckel, *Utility Scale Energy Storage Systems*. West Lafayette, IN, USA: State Utility Forecasting Group, Jun. 2013.

Yingyun Sun (M'14) received the B.S. degree from Shanghai Jiaotong University, Shanghai, China, in 1996, and the M.S. and Ph.D. degrees from Tsinghua University, Beijing, China, in 2004 and 2007, respectively, all in electrical engineering.

He was with Yantai Electric Power Company, Shandong, China, and Tsinghua University. He is currently an Associate Professor with the Electrical Engineering School, North China Electric Power University, Beijing. His current research interests include power system operation, and control and renewable energy integration.

Zuyi Li (SM'09) received the B.S. and M.S. degrees from Shanghai Jiaotong University, Shanghai, China, in 1995 and 1998, respectively, and the Ph.D. degree from the Illinois Institute of Technology (IIT), Chicago, IL, USA, in 2002, all in electrical engineering.

He is currently a Professor with the Electrical and Computer Engineering Department, IIT. His current research interests include economic and secure operation of electric power systems, cyber security in smart grid, renewable energy integration, electric demand management of data centers, and power system protection.

Mohammad Shahidehpour (F'01) received the Ph.D. degree from the University of Missouri, MO, USA, in 1981, and is the recipient of an Honorary Doctorate from the Polytechnic University of Bucharest, Bucharest, Romania.

He is the Bodine Chair Professor and the Director of the Robert W. Galvin Center for Electricity Innovation at the Illinois Institute of Technology, Chicago, IL, USA. He is a Research Professor with King Abdulaziz University, Jeddah, Saudi Arabia, and an Honorary Professor with North China Electric Power University, Beijing, China, and Sharif University, Tehran, Iran.

Dr. Shahidehpour was the recipient of the 2012 IEEE Power and Energy Society (PES) Outstanding Power Engineering Educator Award and the Honorary Doctorate Award from the Polytechnic University of Bucharest, Bucharest, Romania. He is an IEEE Distinguished Lecturer, and the Chair of the 2012 IEEE Innovative Smart Grid Technologies Conference, the 2012 Great Lakes Symposium on Smart Grid, and the New Energy Economy. He is the Editor-in-Chief of the IEEE TRANSACTIONS ON SMART GRID.

Bo Ai received the B.S. degree from North China Electric Power University, Beijing, China, in 2014, and where he is currently pursuing the M.S. degree, both in electrical engineering.